BIODIVERSITAS
Volume 25, Number 2, February 2024
Pages: 846-858

ISSN: 1412-033X
E-ISSN: 2085-4722
DOI: 10.13057/biodiv/d250245

Micromorphology, physicochemical parameters, and phytochemical screening of *Chloranthus flavus* D.T. Liu & G. Chen (syn. *C. nervosus* Collett & Hemsl.) from Vietnam

TRAN VAN CHEN[1,♥], DUONG NGUYEN XUAN LAM[2], HOANG DAC KHAI[3], DUONG PHAN NGUYEN DUC[1], NGUYEN THI NGA[1], NGUYEN THI THU HIEN[4], TRAN THI THUY QUYNH[1,♥♥]

[1]Faculty of Traditional Medicine, University of Medicine and Pharmacy at Ho Chi Minh City. No. 217, Hong Bang Street, Ward 11, District 5, Ho Chi Minh City 700000, Vietnam. Tel./fax.: +84-28-3855-8411, ♥email: tvchenpharma@ump.edu.vn, ♥♥email: thuyquynhtran31@ump.edu.vn
[2]Faculty of Pharmacy, University of Medicine and Pharmacy at Ho Chi Minh City. No. 217, Hong Bang Street, Ward 11, District 5, Ho Chi Minh City 700000, Vietnam
[3]IVFMD Phu Nhuan, My Duc Phu Nhuan Hospital. No. 43R/2-4, Ho Van Hue Street, Ward 9, Phu Nhuan District, Ho Chi Minh City 700000, Vietnam
[4]Faculty of Pharmacy, Nguyen Tat Thanh University. Ho Chi Minh City. No. 300A, Nguyen Tat Thanh Street, Ward 13, District 4, Ho Chi Minh City 700000, Vietnam

Manuscript received: 22 January 2024. Revision accepted: 28 February 2024.

Abstract. *Chen TV, Lam DNX, Khai HD, Duc DPN, Nga NT, Hien NTT, Quynh TTT. 2024. Micromorphology, physicochemical parameters, and phytochemical screening of* Chloranthus flavus *D.T. Liu & G. Chen (syn.* C. nervosus *Collett & Hemsl.) from Vietnam. Biodiversitas 25: 846-858. Chloranthus flavus* D.T. Liu & G. Chen (syn. *C. nervosus* Collett & Hemsl.) is a subshrub belonging to the family Chloranthaceae. Information on the anatomical structure and the powder features of *C. flavus* has not been noted. This study aimed to develop a monograph on the microscopic characteristics and physicochemical parameters of *C. flavus*, as well as a preliminary assessment of the phytochemical composition of this species. Anatomical characterizations of roots, stems, and leaves were performed using the iodine green-carmine staining method and then an optical microscope was used to observe the histology of these parts, similar to observing powder characteristics. Secondary metabolites were detected by chromogenic or precipitation reagents. Anatomically, the structural characteristics of the roots, stems, and leaves are similar to those of the *Chloranthus* species. Particularly, the root structure is characterized by six alternating xylem bundles, with six phloem bundles forming a ring. Polygonal to irregularly shaped cells of the upper epidermis and irregularly shaped ordinary cells, laterocytic and anomocytic stomata types, stomatal clusters, and the stomatal index (15.75±1.52%) of the lower epidermis were observed in leaves. Both powders found fragments of epidermal and parenchymatous cells, spiral xylem vessels, and scalariform xylem vessels. However, the root powder only observed solid-shaped sclereid cells, starch granules, starch clusters, and calcium oxalate crystals. The powders' moisture content, total ash, and acid-insoluble ash values all meet acceptable standards according to regulations on raw material purity. The whole *C. flavus* plant contains carotenoids, fatty acids, essential oils, flavonoids, tannins, coumarins, alkaloids, triterpenoids, amino acids, and carbohydrates. The current findings highlight the key characteristics for identifying *C. flavus*.

Keywords: Anatomical structure, *Chloranthus flavus*, powder feature, pharmacognostic parameters, phytochemistry

Abbreviations: ddw: double distilled water; SI: Stomatal Index; Syn.: Synonym

INTRODUCTION

The Chloranthaceae family consists of four genera: *Ascarina* J.R.Forst. & G.Forst., *Chloranthus* Sw., *Hedyosmum* Sw., and *Sarcandra* Gardner, with more than seventy-three accepted species (POWO 2024a). Among these, *Chloranthus* Sw. is the type genus of the family Chloranthaceae, one of the most primitive plant families that still exists, with the number of accepted species varying from 15 to 17 because of the arguments between taxonomists about the plant's macromorphology (Liu et al. 2019; POWO 2024b; FOC 2024). The genus *Chloranthus* Sw. consists of sub-shrubs or perennial herbs and is widely distributed in the tropical lands of southern and eastern Asia, especially in mainland China (Liu et al. 2022; FOC 2024). Some species of this genus are used in folk medicine due to its biologically active compounds (Guo et al. 2016; Ariffin et al. 2023). According to phytochemical research, the genus *Chloranthus* contains more than 400 bioactive compounds, including terpenoids, coumarins, lignans, amides, phenylpropanoids, flavonoids, organic acids, and other compounds (Liu et al. 2022; Ariffin et al. 2023); in which, sesquiterpenoids and diterpenoids are dominant components (Wang et al. 2015). Pharmacological studies revealed that this genus possesses anti-inflammatory, anti-tumor, neuroprotective, hypoglycemic, antimalarial, hepatoprotective, antibacterial, and antiviral activities (Wang et al. 2015; Liu et al. 2022).

In Vietnam, four species in the *Chloranthus* genus have been recorded as native: *Chloranthus spicatus* (Thunb.) Makino, *Chloranthus erectus* (Buch.-Ham.) Wall. (syn., *Chloranthus elatior* R.Br.), *Chloranthus nervosus* Collett & Hemsl., and *Chloranthus japonicus* Sieb. (syn., *Chloranthus serratus* (Thunb.) Roem. & Schult.) (Thang et

al. 2016; POWO 2024a); in 2022, *C. nervosus* was suggested as a synonym for *C. flavus*, according to the research of Lu et al. (2022). Among the above species, *C. japonicus*, *C. elatior*, and *C. spicatus* have been widely used in folk medicine for the treatment of infection, joint pain, traumatic injuries, rheumatic arthralgia, bone fractures, common cold, fever, high blood pressure, and so on (Thang et al. 2016; Zhuo et al. 2017). There has been no research on the micro-morphological properties and pharmacognostical parameters of the *C. flavus* plant and its synonym until now. In the very first steps of using this plant in the evidence-based medical field, there is a need for botanical identification and standardization of these herbs (WHO 2011; Ministry of Health 2017).

Precise species identification is crucial to search and focus on their various bioactive potentials. The initial and most common approach to taxonomy has historically been describing macro-morphological features because of its ease and convenience (Van Chen et al. 2022). The macro-morphology, or external morphology, is diversed or varied between species in a genus because of various factors, including macromorphological similarity, distinct genetic and morphological variation, and polyploidization and hybridization. Those factors make identifying a species more challenging (Nhi et al. 2023). Meanwhile, micro-morphology plays a vital role in taxonomic identification issues because micro-morphological, morpho-anatomical (the structure of the plant body), histochemical, and powder microscopic features are related to the plant structure and composition (Alamgir 2017; Van Chen et al. 2022). Identifying medicinal plants and standardizing raw medicinal herbs depends heavily on micro-morphological characteristics (Anu et al. 2020). Additionally, the micro-morphological species identification method can circumvent the macro-morphological taxonomy's limitations for closely related species whose characteristics may still lack sufficient basis for differentiation. Therefore, some taxonomists identify species based on the combination of macro-morphological description and micro-morphological analysis (Anu et al. 2020; Nhi et al. 2023).

Moreover, *C. flavus* has been macro-morphological described in detail in the study of Liu et al. (2019), and macromorphologically, *C. flavus* is a sub-shrub, 35-55 cm tall. The rhizome has many fibrous roots, a brown color, and a strong odor. The stem is erect and branched, consisting of 2-5 nodes; each internode is 5-7 cm long; and each node has 1 pair of scale-shaped leaves, ovate-triangular or triangular, with 0.3-0.6×0.2-0.4 cm. The leaves are opposite, consisting of 2 or 4 leaves at the tip of the branch, and whorled. Petioles are 0.5-1.5 cm long, and broad leaf blades are elliptical or ovate, with serrated edges, 7-19×3.5-13 cm. The flowers are yellow. Androecium 3, stamens elongated, straight, 5-8 mm, yellow, confluent at the base. The central connective has a two-chambered anther, and the lateral connectives have a one-chambered anther. The ovary is ovoid-shaped. The fruit is green, black when ripe, obovoid-shaped, and 0.3×0.45 cm (Figure 1) (Liu et al. 2019); however, there is still no study on the micro-morphology of the plant. Therefore, this study provides information on micro-morphological features to identify *C. flavus* harvested in Vietnam precisely. In terms of standardization of herbal medicine, this study performs preliminary phytochemical screening to determine the plant's phytochemical components. Also, this study determined some physico-chemical parameters of the herbs collected in Vietnam, including moisture content, total ash value, and acid-insoluble ash value (Ministry of Health 2017). These results are a reliable document to support the precise identification of *C. flavus* in Vietnam to set a foundation for selecting the correct species as medicinal and motivate further research on isolating purified compounds and determining the pharmacological activities of this medicinal plant.

MATERIALS AND METHODS

Plant material

As botanical material for this study, the fresh plants were collected in the highland area of Lang Bian, Lam Dong province, Vietnam (coordinate 12°00'28.9" N, 108°23'20.8" E) in June 2023. The scientific name of the samples was determined based on the standard method of morphological comparison with photographs and described in references by Liu et al. (2019) and Lu et al. (2022). This specimen's scientific name was *Chloranthus flavus* D.T. Liu & G. Chen (Syn., *C. nervosus* Collett & Hemsl.). A voucher specimen (collector's number: TVC-02.23) was deposited at the Department of Traditional Pharmacy, Faculty of Traditional Medicine, University of Medicine and Pharmacy at Ho Chi Minh City, Ho Chi Minh City, Vietnam. The morphological features of *C. flavus* are presented in Figure 1. Then, the samples were washed thoroughly under tap water for micro-morphological analysis. Part of the samples were dried at room temperature for powder features, physico-chemical parameters, and phytochemical screening analyses.

Procedures of micro-morphological study

Micro-morphological characteristics

The micro-morphological characteristics of the samples were determined according to the guidelines of the Vietnamese Pharmacopoeia V (Ministry of Health 2017) via the double staining method of iodine green-carmine. Briefly, the various organs (leaves, roots, and stems) of *C. flavus* were chopped and cut into segments/pieces with a razor. The samples were then manually cut horizontally into thin slices (approximately 10-20 μm thick) with a razor blade. Next, the thin finished cross-sections were bleached with 5.0% (w/v) chloramine-T detergent and followed by 50% (v/v) chloral hydrate for 10 min. Those slices were neutralized with 1.0% (w/v) acetic acid for 2 min before being double stained with 0.3% (w/v) Iodine Green and 1.0% (w/v) Carmine, in which the sample was immersed in Iodine Green for 5s and in Carmine for 10s (until the samples became clearer). After each step, excess bleach, reagents, and dyes were removed using double distilled water (ddw). Samples were placed on slides with 1-2 drops

of the glycerin-water mixture (50:50, v:v) pre-existing and covered with a coverslip. The samples were observed and photographed under an optical microscope (Labomed, USA) at 4×, 10×, and 40× magnifications. Similarly, the leaf and rhizome powder features were also observed under the microscope with 10X and 40X magnification (Labomed, USA) (Ministry of Health 2017; Van Chen et al. 2022).

For the leaf epidermal surface feature, the stomata, and the stomatal index (SI) analysis, the fresh leaves of *C. flavus* were collected and manually separated from the leaves' upper and lower epidermis. Epidermal samples were placed on slides with 1-2 drops of distilled water and covered with a coverslip; then, the samples were observed under an optical microscope (Labomed, USA) with a magnification of 40× (WHO 2011; Van Chen et al. 2022). Moreover, SI was determined according to the formula (with 20 replicates) (Ministry of Health 2017; Van Chen et al. 2022).

The stomatal index (SI) is an important value for plant classification and supports the accurate identification of species (Van Chen et al. 2022 Determination of SI done by the formula (at 40× magnification): SI (%) = (S/(S+E)) × 100. Where S and E are the numbers of stomata and epidermal cells (including trichomes) in the observable field of view by microscopy at 40X magnification (Labomed, USA), respectively (Van Chen et al. 2022).

Procedures of phytochemical study

Pharmacognostic evaluation

Cloranthus flavus roots and aerial parts were washed and air-dried until the raw sample maintained less than 13.0% moisture content. In the next step, the samples were ground into separate powders to evaluate the physicochemical parameters of medicinal raw materials. In other words, the moisture content, total ash value, and acid-insoluble ash value were performed according to the Vietnamese Pharmacopeia V standard procedure (Ministry of Health 2017; Van Chen et al. 2022).

Figure 1. *Chloranthus flavus* plant collected in Vietnam. A. The whole plants; B. Inflorescence and flower; C. Fruits

Preparation of extracts and preliminary phytochemical screening

Plant secondary metabolites were identified using standard protocols described by Iqbal et al. (2015) and Tran et al. (2023), with minor modifications. Briefly, the dried powder samples (50 g root and 50 g aerial part) were extracted by soaking (ultrasonic extraction) in 100 mL of 96% ethanol for 30 min at 45°C. After that, these extracts were tested for phytochemical components, including carotenoids, fatty acids, essential oils, flavonoids, tannins, coumarins, alkaloids, triterpenoids, steroids (cardiac glycosides), saponins, amino acids, and carbohydrates. These experiments were repeated in triplicate under the same conditions (Iqbal et al. 2015; Tran et al. 2023).

Data analysis

Micro-morphological measurement was made using an eyepiece micrometer scale (Olympus, Japan) and a standard ruler to determine the sizes of the sample parts and cell components. The stomatal number was counted 20 times, and the resulting data was used to calculate the stomatal index (SI). Using Microsoft Excel 2023, all findings were analyzed and presented as mean values with SD (Standard Deviation) (WHO 2011; Van Chen et al. 2022; Nhi et al. 2023).

RESULTS AND DISCUSSION

Micro-morphological characters

Anatomical features

Roots. The cross-section of the roots is nearly circular. From the outside to the inside, it is composed of two regions: the cortex region (which accounts for 2/3 of the cross-section) and the stele region (which accounts for 1/3 of the cross-section) (Figure 2A). (i) The cortex region: The outermost layer consists of a single layer, polygonal cells, and cellulose walls called the epidermis (hair-root layer) (Figure 2a). The next layer is a suberin-impregnated layer (suberized hypodermal cells) consisting of one layer, polygonal cells, and lignified cell walls (Figure 2b). The cortical parenchyma region consists of many layers, nearly round polygonal cells, thin cellulose walls, and cells randomly arranged to form triangular or polygonal intercellular spaces (Figures 2c and 2d). Polygonal crystal fibers with very thick lignified cell walls are abundant in the cortical parenchyma region (Figure 2e).

(ii) The stele region: This region includes endodermis, pericycle, vascular bundles (xylem and phloem), parenchymatous rays, and parenchymatous pith. The endodermis is a single-layer Casparian strip with polygonal cells (Figure 2f). The next layer is the pericycle (Figure 2g), consisting of a single layer, polygonal cells, and cellulose walls interspersed with endodermal cells. For the characteristics of vascular bundles, especially six xylem bundles (star-shaped) (Figure 2h), they are arranged alternately with six phloem bundles and arranged in a ring. Each xylem bundle has 5-6 vessels, polygonal xylem vessels, lignified cell walls, and radial differentiation (Figure 2h). Phloems are polygonal cells with cellulose walls, randomly arranged in clusters (Figure 2i). Ray parenchyma comprises 1-2 rows of polygonal cells with lignified cell walls (Figure 2j). The parenchymatous pith is multi-layered, with polygonal cells, slightly thickened lignified cell walls that tend to turn into sclerenchymatous tissues, and random arrangement without intercellular spaces (Figure 2k).

Stems. Anatomically, the cross-section of the stem is approximately circular (Figure 3A). The structure of the stem includes the following layers: The epidermis is a layer of polygonal cells covered by a flat and thin cutin layer with cellulose-impregnated cell walls (Figure 3a). The next layer is the thickness-angular collenchymatous cells, comprising 2-3 layers (Figure 3b). The collenchyma tissues are polygonal cells with cellulose-impregnated cell walls arranged randomly (Figure 3b). The cortical parenchyma has many layers with nearly round polygonal cells, thin cellulose cell walls, and triangular or polygonal intercellular spaces (Figures 3c and 3d). The pericycle is sclerotically transformed into a continuous ring of 1-2 layers with polygonal cells and slightly thick lignified cell walls (Figure 3e). Phloem consists of polygonal cells with slightly curved cellulose-impregnated cell walls and a random arrangement (Figure 3f). Each xylem bundle comprises 6-8 polygonal vessels with lignified cell walls (Figures 3g and 3g'). The xylem parenchyma comprises polygonal cells with lignified cell walls (Figure 3g'). The parenchymatous ray includes 2-3 rows with polygonal cells and lignified cell walls (Figure 3h). The parenchymatous pith region comprises many nearly round cell layers with thin cell walls and triangular or polygonal intercellular spaces (Figures 3i and 3j). Scattered oil cells (Figure 3k) and cuboidal or square-shaped calcium oxalate (Figure 3l) were also found in this region.

Leaves. (i) Midrib, vascular bundles, and leaf blade. The cross-section of the leaf is V-shaped, consisting of two structural parts: the midrib and the leaf blade. The midrib area is also approximately five times larger than the leaf blade area (Figure 4A).

(ii) Midrib region (Figure 4A): The upper surface is concave, and the lower surface is more convex. The upper and lower epidermis consist of one layer covered by a thin layer of serrated cuticle with polygonal cells and cellulose walls (Figures 4a, 4b, and 4c). The upper and lower angular collenchymas consist of 2-3 and 4-5 layers, respectively, which are randomly arranged with polygonal cells and thickened cellulose walls (Figures 4d and 4e). Parenchyma cells are multi-layered, nearly round cells with thin cellulose walls randomly arranged to form triangular or polygonal intercellular spaces and scattered with oil cells (Figures 4f, 4g, and 4h). The vascular bundle system is arranged to form a nearly continuous arc with the xylem above and the phloem below. The xylem has a polygonal shape and lignified walls, gradually increasing in size from upper to lower; each row has 3-6 xylem vessels (Figure 4i). The xylem parenchyma comprises polygonal, thin-walled cellulose cells arranged in rows and interspersed with rows of xylem (Figure 4j). Phloem comprises polygonal cells with thin, slightly curved cellulose walls randomly arranged in clusters (Figure 4k).

(iii) Leaf blade region (Figure 4D): The upper and lower epidermis comprises one layer covered by a thin layer of serrated cuticle, polygonal cells, and cellulose walls (Figure 4a). The upper epidermal cells are larger than the lower ones, and stomata are only concentrated in the lower epidermis (Figure 4n). The mesophyll has an asymmetrical heterostructure; the spongy parenchyma is 4-5 times larger than the palisade parenchyma. The palisade parenchyma has a single layer with polygonal cells arranged at right angles to the upper epidermis (Figure 4l). The spongy parenchyma consists of randomly arranged layers of polygonal cells (Figure 4m). In addition, scattered obliquely cut sub-vascular bundles were observed (Figure 4o).

Epidermal cells, stomata, and stomatal index. The arrangement of the upper epidermal cells was consistently more regular than that of the lower epidermal cells (Figure 5). The lower epidermis was usually composed of polygonal cells with deeply curved or arched walls arranged haphazardly with irregular sizes between cells (Figure 5A). In general, the lower epidermal cells have an elongated size, with a length (L) being about 1.9 times longer than a width (W) for larger epidermal cells and about 3.7 times longer for smaller epidermal cells (Figures 5A and 5f). Similarly, the upper epidermis also had elongated or oval polygonal cells, and straight or arched walls, with a length (L) approximately 1.45 times longer than a width (W) (Figures 5B and 5g). The sizes (L × W) of upper and lower epidermal cells were 39.25±2.99 × 27.0±2.45 μm and 87.50±6.45× [(24.0±3.37)-(46.50±3.11)] μm, respectively. Moreover, the lower epidermal surface was scattered with red-brown resin masses (Figure 5i). The costal epidermal cells consist of 4-5 layers of polygonal cells that continuously elongate vertically, with the cell length (42.5±6.45 μm) being much greater than its width (14.25±1.71 μm) (Figure 5h).

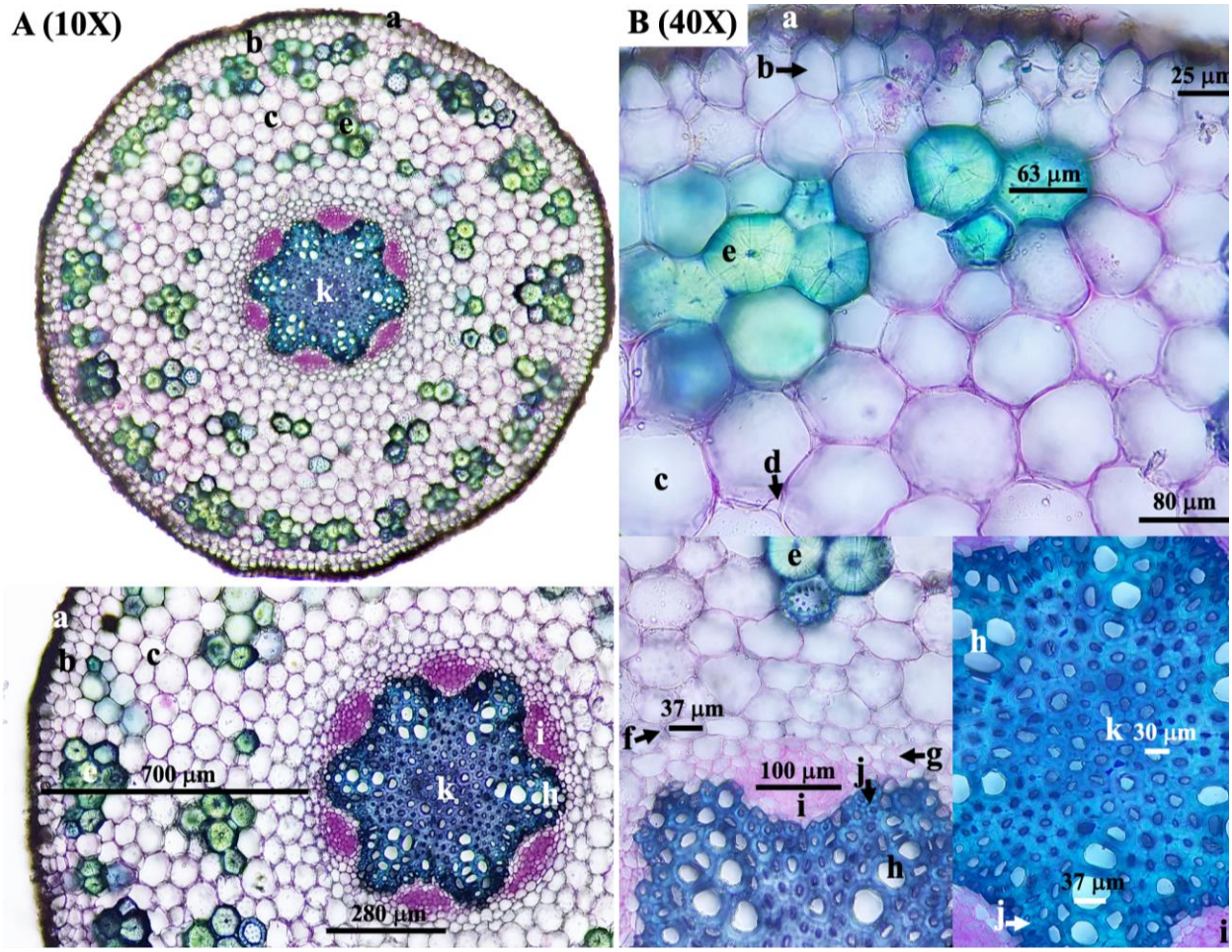

Figure 2. The features of the cross-sectioned root of *C. flavus* (with magnifications A. 10X; and B. 40X). a. Epidermis; b. Suberin-impregnated layer (suberized hypodermal cells); c. Parenchymatous cells of the cortex region; d. Triangular or polygonal intercellular spaces; e. Polygonal crystal fibers; f. Endodermis with casparian strip; g. Pericycle; h. Xylem and xylem vessels; i. Phloem; j. Parenchymatous ray; k. Parenchymatous pith

The type of stomata is laterocytic, with three or more lateral subsidiary cells around the stoma pore. In other words, the stomatal apparatus consists of three or more lateral subsidiary cells (polygonal) located around the guard cells (reniform), forming a wide ellipse (L × W, 50.25±1.71×32.75±2.22 µm) (Figures 5A and 5a, red arrow). Furthermore, anomocytic stomata (Figure 5d, red circle) are also found in this species but are less observable than laterocytic stomata. In particular, stomatal clusters are observed only on the lower epidermal surface. These stomatal clusters consist of 2-3 stomata and two stomata arranged adjacent to each other through a lateral subsidiary cell (Figure 5d). The stomatal apparatus is also observed only on the epidermis's lower surface and not found on the upper surface. The absence of trichomes (hairs) was also noted on both epidermal surfaces (Figure 5). Therefore, the stomatal index (SI) is calculated for the lower leaf surface to be 15.75±1.52 (%).

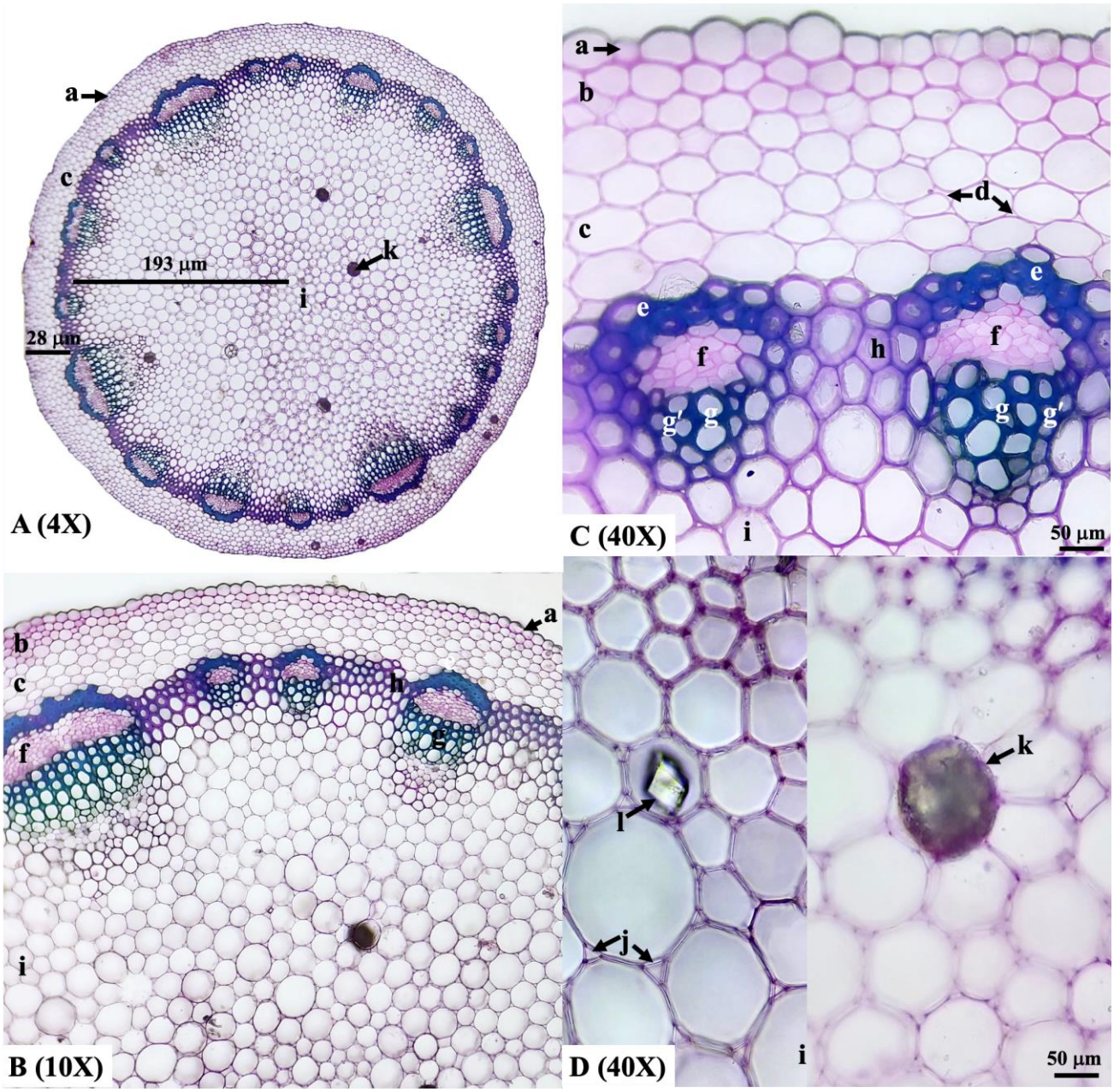

Figure 3. The features of cross-sectioned stem of *C. flavus* (with magnifications 4X, 10X, and 40X): a. Epidermis with flat and thin cutin layer; b. Thickness-angular collenchymatous cells of the cortex region; c. Parenchymatous cells of the cortex region; d. Triangular or polygonal intercellular spaces; e. Pericycle (transforms into a sclerenchymatous bundle sheath); f. Phloem; g,g'. Xylem, xylem vessels, and xylem parenchyma; h. Parenchymatous ray; i, j. Parenchymatous cells with intercellular spaces of the pith region; k. Oil cell; l. calcium oxalate

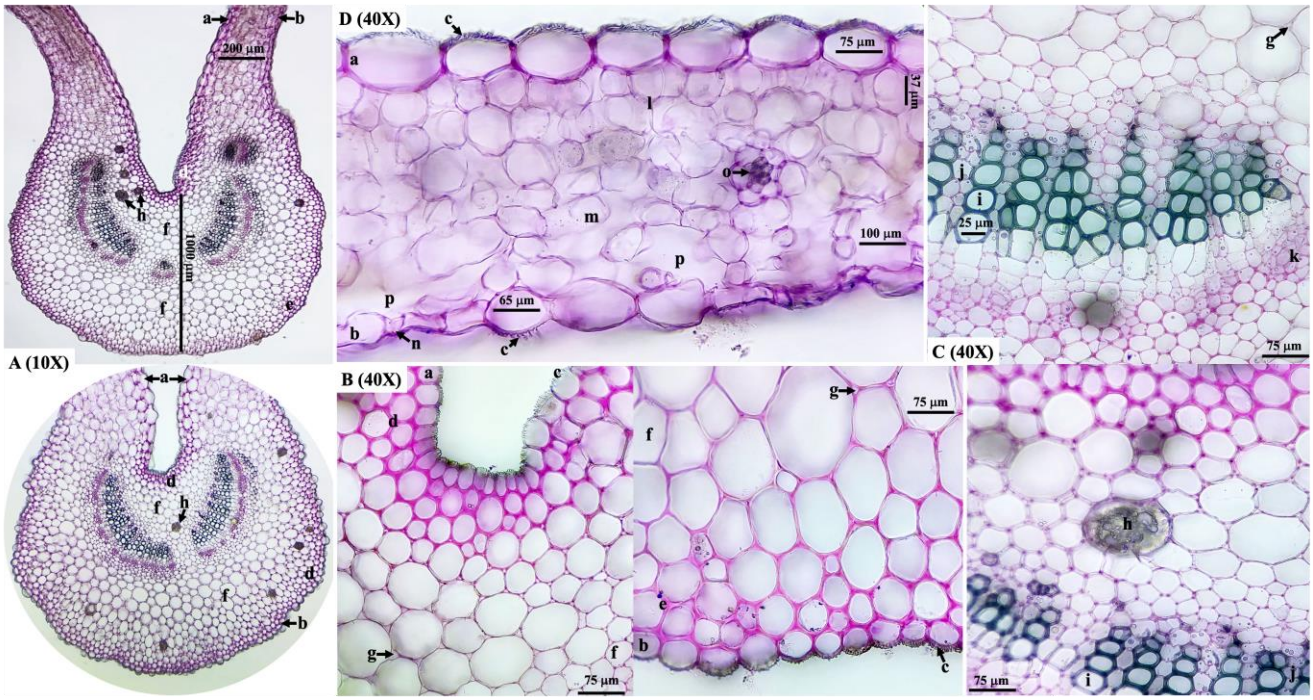

Figure 4. The features of cross-sectioned leaves of *C. flavus* (with magnifications 10X and 40X): a. Upper epidermis; b. Lower epidermis; c. Thin serrated cuticle layer; d. Upper collenchymatous cell; e. lower collenchymatous cell; f. Parenchymatous cell; g. Triangular or polygonal intercellular spaces; h. Oil cell; i. Xylem and xylem vessels; j. Xylem parenchyma; k. Phloem; l. Palisade parenchyma; m. Spongy parenchyma; n. Lower stomata; o. Sub-vascular bundles; p. Sub-stomatal cavity

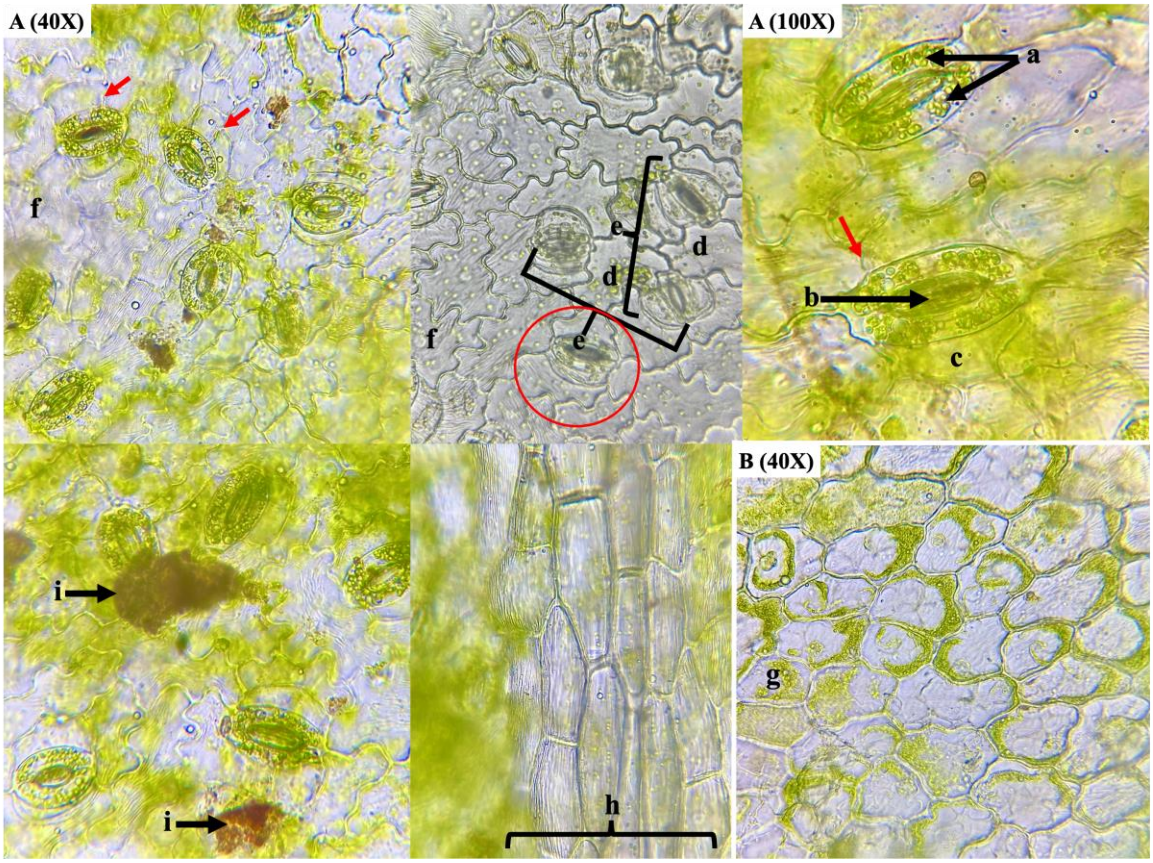

Figure 5. Epidermis with stomata of *C. flavus* (with magnifications 40X and 100X): A. Lower surface view of the epidermis with stoma closed/opened; B. Upper surface view of the epidermis; a. Guard cells; b. Stomatal pore; c,d. Lateral subsidiary cells; e. Stomatal clusters; f. Lower epidermal cells; g. Upper epidermal cells; h. Costal epidermal cells; i. Red-brown resin masses

Powder features

Root powders. The sensory properties of the root powder are characterized by its yellow-brown or dark-brown color, strong smell, and tastelessness (Figure 6A). The components of the root powder, including the fragment of epidermal cells (Figure 6B), the fragment of parenchymatous cells (Figure 6C), the sclereid cells (Figure 6D), the starch granules, the starch clusters, the calcium oxalate crystals, the red-brown oleoresin masses (Figure 6E), the fragment of brown cork (Figure 6F), the fragment of spiral xylem vessel (Figure 6G), the fragment of scalariform xylem vessel (Figure 6H), and the needle-shaped coumarin crystals (Figure 6I), were observed through the field of view.

Stem and leaf powders. Organoleptically, the leaf powder is characterized by its dark green color, slightly strong odor, and slightly bitter taste (Figure 7A). Through microscopic observation, the presence of ingredients such as the fragment of epidermal cells (Figure 7B), the fragment of dark-brown corky epidermis (Figure 7C), the fragment of parenchymatous cells with stomata (Figure 7D), the fragment of parenchymatous cells with round-green chloroplasts (Figure 7E), the fragment of red-brown resin masses or clusters (Figure 7F), the fragment of spiral xylem vessel (Figure 7G), the fragment of scalariform xylem vessel (Figure 7H), the thick-walled bundle of fibers (Figure 7I), and thick-walled sclereid fiber (Figure 7J) were found in the stem and leaf powder. Generally, the components observed in aerial part powder and fresh are similar in ingredients. Furthermore, the upper and lower epidermis present in the leaf powder can be distinguished via stomata-bearing epidermal or parenchymal cell fragments because stomata are found only in the lower epidermis.

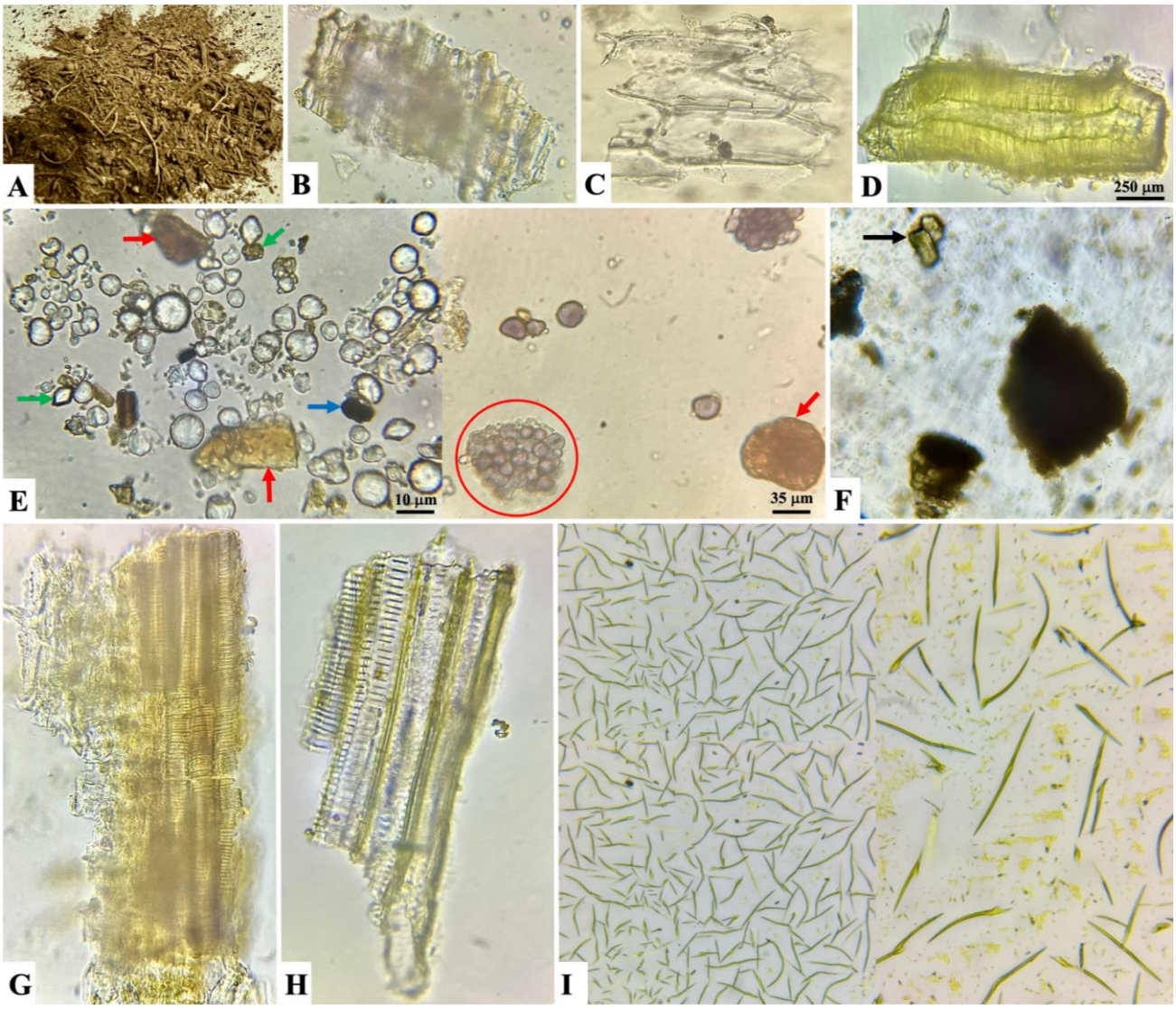

Figure 6. The features of *C. flavus* root powder (with magnifications 40X): A. Root powders; B. Fragment of epidermal cells; C. Fragment of parenchymatous cells; D. Sclereid cells (solid shape, black arrow); E. Starch granules (polygonal-shaped or pear-shaped); Starch cluster (stained with iodine-potassium iodide reagent, purple-blue, red circle), calcium oxalate crystals (solid shape, green arrow), and red-brown oleoresin masses (red arrows); F. Fragment of brown cork (blue arrow); G. Fragment of spiral xylem vessel; H. Fragment of scalariform xylem vessel; I. Needle-shaped coumarin crystals (micro-sublimation reaction of coumarins)

Phytochemical and physico-chemical evaluations

Phytochemical screening

Secondary metabolites were present in the root and aerial part extracts, including carotenoids, fatty acids, essential oils, flavonoids, tannins, coumarins, alkaloids, triterpenoids, amino acids, and carbohydrates. However, saponin and cardiac glycoside compounds were not detected in the plant extracts under the analysis conditions. The results of the preliminary phytochemical screening of *C. flavus* extracts are presented in Table 1.

Physico-chemical parameters

The moisture content, total ash value, and acid-insoluble ash value of the root and aerial part powders from *C. flavus* were measured in triplicate (n=3). The average results of moisture content, total ash value, and acid-insoluble ash value are 11.65±0.72% (w/w), 9.83±0.30% (w/w), and 0.53±0.06%, respectively, for the root powder, followed by 11.36±0.87% (w/w), 7.80±0.32% (w/w), and 0.39±0.05%, respectively, for the aerial part powder.

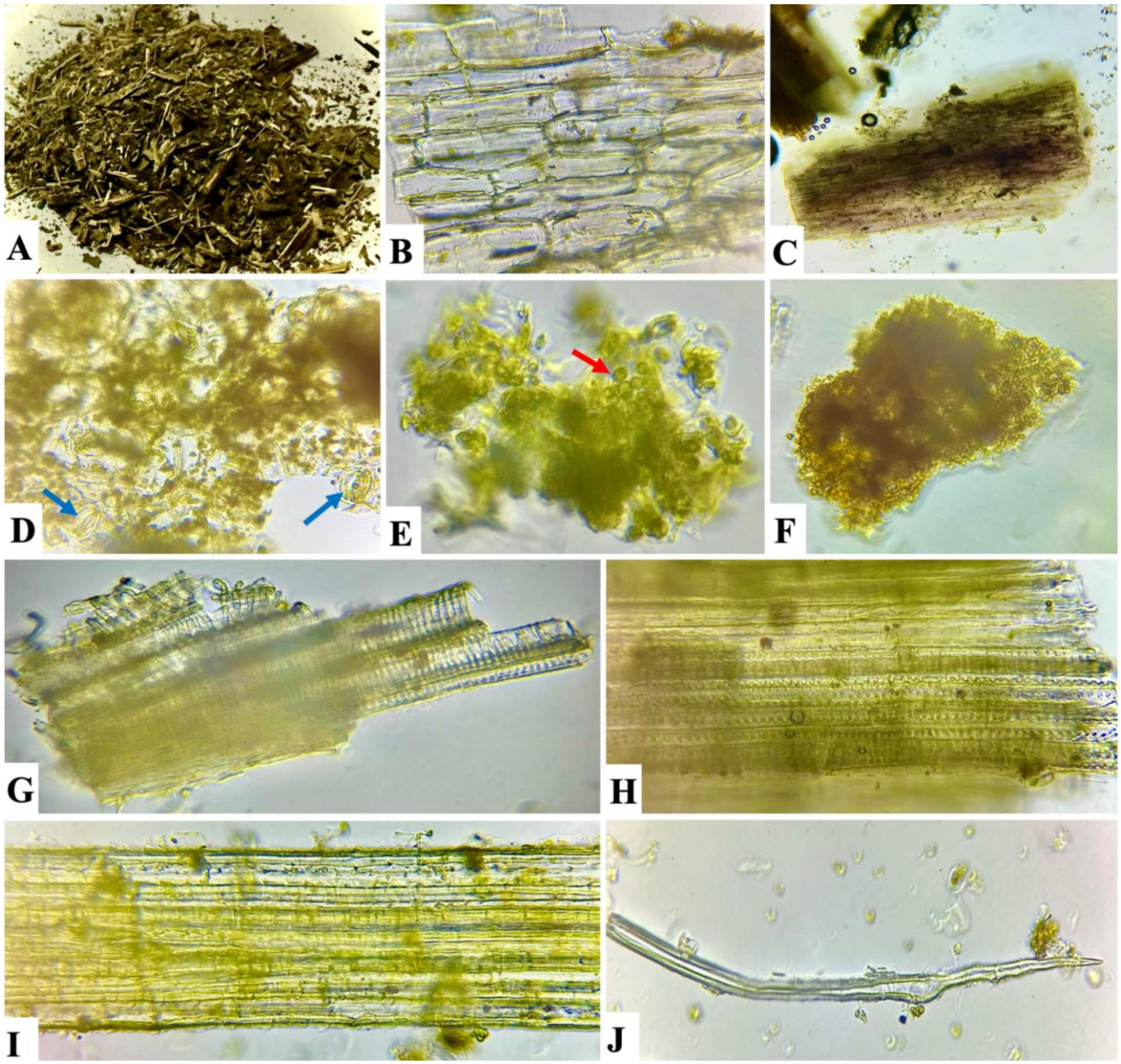

Figure 7. The features of dried aerial part powder of *C. flavus* (with magnifications 40X): A. Stem and leaf powder; B. Fragment of epidermal cells; C. Fragment of dark-brown cork; D. Fragment of parenchymatous cells with stomata (blue arrow); E. Fragment of parenchymatous cells with round-green of chloroplasts (red arrow); F. Fragment of red-brown resin masses (gather together into resin clusters); G. Fragment of spiral xylem vessel; H. Fragment of scalariform xylem vessel; I. Thick-walled bundle of fibers; J. Thick-walled sclereid fiber

Table 1. Preliminary phytochemical screening of roots and aerial parts of *C. flavus*

Phytocompounds	Test	Inference	
		The root extract	The aerial part extract
Carotenoids	H_2SO_4 test	+	+
Fatty acids	Stain test	+	+
Essential oils	Scent test	+	+
Polyphenols	$FeCl_3$ 1% test	+	+
Flavonoids	Shinoda (Cyanidin) test	+	+
Tannins	Gelatin's test	+	+
Coumarins	Microsublimation test, Lactone ring test	+	+
Alkaloids	Valse-mayer's test, Bouchardat's test, Dragendoff's test	+	+
Triterpenoids	Salkowski test	+	+
Steroid/Cardiac glycosides	Liebermann Burchard test/ Raymond's test, Xanthydrol's test	-	-
Saponins	Foam test	-	-
Amino acids	Na_2CO_3 test	+	+
Carbohydrates	Molisch's test, Fehling's test	+	+

Notes: "+" and "-" indicate the presence and absence of the phytochemical constituents, respectively

Discussion

Along with the morphological identification method, the anatomical method is probably the one that has been used for a long time to confirm botanical identification. These methods are still considered effective and accurate. By identifying important anatomical features of plants, taxonomists can properly authenticate plant specimens and detect any confusion that may have occurred (WHO 2011; Osman et al. 2019). Previous studies reported that the sensory method was used to observe herbal powders' characteristic color, odor, or taste through the senses of sight, smell, or taste (Osman et al. 2019). This is considered a quick and inexpensive method of observing samples and combined with a microscope to preliminary check the purity of raw powders. In other words, using a microscope is a quick tool to identify plants anatomically (i.e., the features of plant tissue) and to test the accuracy and purity of powders due to intentional or unintentional adulteration (WHO 2011; Alamgir 2017; Srivastava et al. 2018; Osman et al. 2019). The roots, stems, and leaves of *C. flavus* were described in detail using microscopy to highlight their important anatomical features.

Anatomically, the major characteristics of *C. flavus* leaf, including the epidermis layer, thin serrated cuticle layer, collenchymatous/parenchymatous cells, palisade parenchyma, spongy parenchyma, and sub-stomatal cavity, have many similarities with other species of the same *Chloranthus* genus (e.g., *Chloranthus multistachys* Pei (Li et al. 2011), *C. japonicus* (Kang et al. 2010); etc.). In addition, the absence of trichomes on both leaf surfaces and stomata only in the lower leaf epidermis was also observed in both *C. flavus* and other species of the genus *Chloranthus* (e.g., *C. multistachys* (Li et al. 2011), *C. japonicus* (Kang et al. 2010), *C. spicatus*, *C. erectus*. (= *C. officinalis* Blume), *Chloranthus sessilifolius* K.F.Wu (Kong et al. 2001); etc.

Overall, the anatomical structures of the *C. flavus* root and stem are similar to that of other species of the *Chloranthus* genus (e.g., *C. multistachys* (Li et al. 2011), *C. japonicus* (Kang et al. 2010), and *C. serratus* (Carlquist 1992)), such as the epidermis, cortex region, and stele region. A sclerenchymatous bundle sheath surrounded the stem phloem, a feature also observed in *C. flavus*, *C. multistachys* (Li et al. 2011), and *C. japonicus* (Kang et al. 2010). Additionally, scalariform xylem vessels (i.e., scalariform perforation plates) in the stem and leaf of *C. flavus* are also found in some *Chloranthus* species, such as *C. erectus*, *C. japonicus*, *C. serratus*, and *C. multistachys* (Carlquist 1992).

Per the guidelines for quality control of medicinal plants in the Vietnamese Pharmacopoeia V (Ministry of Health 2017) and WHO (WHO 2011; Alamgir 2017), the stomata type of leaf epidermis is often a rather stable characteristic of a species. Therefore, the number and type of stomata are important for classifying species of the four genera in the family Chloranthaceae. Stomata are the respiratory pores of cells on the leaf surface that exchange gases and limit water loss due to transpiration (Nunes et al. 2020).

Based on the stomatal architecture (i.e., the number and arrangement of subsidiary cells), Carpenter (2005) classified the main five types of stomata in basal angiosperms, including paracytic types (brachyparacytic, amphibrachyparacytic, holoparacytic, hemiparacytic, and weakly brachyparacytic types), laterocytic types (laterocytic 1+2, laterocytic 2+2, latero-cyclocytic, and weakly laterocytic types), stephanocytic types (stephanocytic, actinocytic, actino-stephanocytic, stephanocytic bicyclic/incomplete stephanocytic bicyclic, and weakly stephanocytic/actinocytic types), anomocytic type, and irregular types (irregular-incomplete laterocytic and irregular-polar types) (Carpenter 2005).

In the present study, only the underside of *C. flavus* (= *C. nervosus*) leaves has the laterocytic and anomocytic types of stomata, consistent with that reported by Kong (2001). In particular, these types of stomata are also observed in many different species, such as *C. angustifolius* Oliv., *C. japonicus*, and *Chloranthus fortunei* (A.Gray) Solms (Kong 2001). However, *C. multistachys* (Li et al. 2011) and *C. japonicus* (Kang et al. 2010) were only identified as an anomocytic stomatal type.

A comparative study of the stomatal apparatus also showed that the paracytic type was found in the leaves of *C. spicatus*, *C. erectus*, *C. serratus*, *C. sessilifolius*, *C. oldhamii* Solms, and *C. henryi* Hemsl., while the encyclocytic type was present in *C. serratus* but absent in those of *C. flavus* (Kong et al. 2001; Eklund et al. 2004). In particular, our research has found that the stomatal cluster in *C. flavus* leaves consists of 2-3 stomatal apparatuses, each connecting through a lateral subsidiary cell. Segev et al. (2015) suggested that the stomatal index correlates with actual photosynthetic rate and that the stomatal index varies among species of different genera and families. Our present results indicate that the stomatal index (SI) on the lower surface of the leaves from *C. flavus* (15.75±1.52%; = *C. nervosus* 17.50%) can be clearly distinguished from various species of Chloranthaceae, such as *Sarcandra glabra* (Thunb.) Nakai (10.50%), *Sonneratia hainanensis* (C.Pei) Swamy & I.W.Bailey (14.30%), *C. spicatus* (20.10%), *C. erectus* (12.30%), *C. serratus* (19.0%), *C. sessilifolius* (14.90%), *C. oldhamii* (21.50%), *C. henryi* (11.10%), *C. angustifolius* (15.30%), *C. japonicus* (13.40%), *C fortunei* (13.10%), *Hedyosmum orientale* Merr. & Chun (14.30%), *Hedyosmum mexicanum* C.Cordem. (12.90%), *Ascarina lucida* Hook.f. (12.80%), and *Ascarina lanceolata* Hook.f. (12.50%) (Kong 2001). These characteristics are evidence to identify or differentiate *C. flavus* from other *Chloranthus* species. Combining the results of the current study with previous studies (Kong 2001; Carpenter 2005; Lu et al. 2022) on the characteristics of the leaf, including epidermal cells, stomata, and stomatal index, the present study has established the key to classifying some species of the Chloranthaceae family.

Based on microscopy, micro-morphology characterization analysis of raw powders has the advantage of allowing analysis of raw powders at the cellular level and is more suitable for preliminary plant species identification, verification of adulteration, or tampering with powders for fraudulent purposes (Alamgir 2017; Srivastava et al. 2018; Muyumba et al. 2021). As a result of our study on the characteristics of *C. flavus* root and aerial part powders, fragments of epidermal and parenchymatous cells, fragments of spiral xylem vessels, and fragments of scalariform xylem vessels were found in both of these powders. However, components, including solid-shaped sclereid cells, starch granules, starch clusters, and calcium oxalate crystals, were observed in the root powder but not in the leaf powder. In contrast, components such as fragments of parenchymatous cells with stomata and chloroplasts were only found in the leaf powder of this species. This is consistent with the anatomical structure of the leaf as presented in this study. The ingredients contained in this raw powder will assist in identifying intentional or unintentional adulteration for fraudulent purposes. This is the first time raw powders' characteristics have been established as monographic criteria for distinguishing or identifying powders of *C. flavus*.

Key to species

1. Smooth cuticular membrane and invisible wax ornamentation of the upper epidermis; smooth cuticular membrane, suborbiculate-shaped guard cells, not raised outer stomatal rims, absent peristomatal rims of the lower epidermis, and paracytic, laterocytic, encyclocytic types of stomata…..……..*Sarcandra*.
   1a. SI (10.5%)……..*S. glabra*.
   1b. SI (14.3%)……..*S. hainanensis*.
2. Smooth cuticular membrane, irregularly-shaped cells, and invisible wax ornamentation of the upper epidermis; smooth cuticular membrane, wide elliptic-shaped guard cells, stephanocytic type, not raised outer stomatal rims, and absent peristomatal rims of the lower epidermis……*Hydyosmum*.
   2a. Irregular-shaped ordinary cells, SI (14.3%) of the lower epidermis..……..*H. orientale*.
   2b. Polygonal-shaped ordinary cells, SI (12.9%) of the lower epidermis……..*H. mexicanum*.
3. Smooth cuticular membrane and flakes wax ornamentation of the upper epidermis; insular cuticular membrane, suborbiculate-shaped guard cells, raised outer stomatal rims, and present peristomatal rims of the lower epidermis…..…… *Ascarina*.
   3a. Encyclocytic and stephanocytic types of stomata; SI (12.8%)……..*A. lucida*.
   3b. Encyclocytic type of stomata; SI (12.5%)……..*A. lanceolata*.
4. Striate cuticular membrane and invisible wax ornamentation of the upper epidermis; striate cuticular membrane, wide elliptic-shaped guard cells, raised outer stomatal rims, and present peristomatal rims of the lower epidermis……..*Chloranthus*.
   4a. Irregularly-shaped cells of the adaxial epidermis; repand-shaped ordinary cells of the lower epidermis ……..……5.
      5a. Paracytic type of stomata; SI (20.1%)……..……*C. spicatus*.
      5b. Paracytic type of stomata; SI (12.3%)……..……..*C. erectus* (= *C. officinalis*).
      5c. Paracytic and laterocytic types of stomata……6.
         6a. SI (14.9%)……*C. sessilifolius*.
         6b. SI (21.5%)……*C. oldhamii*.
         6c. SI (11.1%)……*C. henryi*.
      5d. Paracytic, laterocytic, and anomocytic types of stomata……7.
         7a. SI (15.3%)……*C. angustifolius*.
         7b. SI (13.4%)……*C. japonicus*.
         7c. Sinuous of anticlinal walls, SI (13.1%)……*C. fortunei*.
   4b. Polygonal to irregularly-shaped cells of the upper epidermis; irregularly-shaped ordinary cells, laterocytic and anomocytic types of stomata, stomatal clusters, SI (15.75±1.52%) of the lower epidermis…..……..*C. flavus* (= *C. nervosus*).

Note: Key-based on the characteristics of the leaf for the taxonomic identification of some plant species belonging to the Chloranthaceae family

In general, the main phytochemical compounds such as triterpenoids, flavonoids, tannins, coumarins, alkaloids, organic acids, fatty acids, and essential oils present in *C. flavus* roots and aerial parts are also found in other *Chloranthus* plants (e.g., *C. japonicus*, *C. fortunei*, *C. angustifolius*, *C. spicatus*, *C. holostegius* (Hand.-Mazz.) C.Pei & San, *C. multistachys*, etc.) (Zhang et al. 2016; Zhuo et al. 2017; Chang-heng et al. 2020; Liu et al. 2022; Wang et al. 2022). In a recent review of the genus *Chloranthus*, Liu et al. (2022) reported that 418 secondary metabolites were isolated from several *Chloranthus* species, including terpenoids, coumarins, lignans, phenylpropanoids, flavonoids, amides, organic acids, and so on (Liu et al. 2022). Previous pharmacological reports of *Chloranthus* species have shown various modern pharmacological properties, including anti-tumor, anti-cancer, anti-inflammatory, antibacterial, antiviral, anti-malarial, neuroprotective, and hypoglycemic activities (Zhang et al. 2016; Zhuo et al. 2017; Chang-heng et al. 2020; Liu et al. 2022; Wang et al. 2022). These pharmacological effects are due to the biologically active groups of active ingredients that are identified in the *Chloranthus* species (Zhang et al. 2016; Liu et al. 2022). Therefore, phytochemical screening was performed in this study as a first step to guide in-depth studies to isolate these secondary compounds as well as their promising pharmacological effects in *C. flavus*.

The moisture content of raw herbs is the cause of chemical changes, enzyme activity, or microbiological infection (Mrozek-Szetela et al. 2020). The result of this situation is damaged medicinal materials that are contaminated with toxins as well as low-quality raw materials. The ideal moisture content of dried medicinal herbs is below 12.0%, or depending on the type of medicinal herb, the pharmacopoeias or other monographs have separate regulations, but the moisture content also fluctuates by less than 13.0% (Ministry of Health 2017; WHO 2011, 2018). In order to ensure medicinal quality, the moisture content in the aerial part and root powders of *C. flavus* of 11.36±0.87% and 11.65±0.72%, respectively, was recorded in our study. This humidity condition meets the general standards prescribed by the Vietnamese Pharmacopoeia V (Ministry of Health 2017) and WHO (2011, 2018).

The components contained in total ash include silicate, silica, carbonate, and phosphate salts. A high total ash value is a sign of contamination, tampering, adulteration, improper manipulation, or handling of the sample. Acid-insoluble ash is a sign of silica pollution, the main source of which is contamination with mechanical impurities such as gravel, sand, and soil (Van Chen et al. 2022, Luan et al. 2022). It will be possible to identify contaminated elements and other components that are absent from the raw herbal material's natural ash by comparing these ash values to the sample's overall ash values (Kaskoos et al. 2014). In our present study, the results showed that total ash values present high values in *C. flavus* aerial part powder (7.80±0.32%) and root powder (9.83±0.30%). Therefore, the total ash value in the roots is higher than that in the aerial parts. This is consistent with observations on their anatomical and powder characteristics, such as crystal fibers, calcium oxalate crystals, etc. Additionally, the acid-insoluble ash values present in root powder (0.53±0.06%) and aerial part powder (0.39±0.05%) indicate low levels of acid-insoluble inorganic constituents in that material (Ministry of Health 2017; Van Chen et al. 2022; Luan et al. 2022). These physico-chemical results are important in determining and evaluating the purity of raw powder from the *C. flavus* plant. Moreover, these physico-chemical parameters can be used to build a monograph to evaluate the quality of the raw powder from this plant. In short, the literature on the anatomical structure and the micro-morphological characteristics of the raw powder from some species of the genus *Chloranthus* is still limited. More in-depth research is needed to gain more information about the anatomical structure of this genus.

In conclusion, the anatomical features of roots, stems, and leaves, as well as the characteristics of the raw powder of *C. flavus*, were reported for the first time in the current study. *C. flavus* is easily distinguished micromorphologically by its root microstructure, which consists of six star-shaped xylem bundles arranged alternately with six phloem bundles forming a ring, followed by a leaf microstructure with polygonal to irregularly shaped cells of the upper epidermis and irregularly shaped ordinary cells, laterocytic and anomocytic stomata types, stomatal clusters, and the stomatal index (15.75±1.52%) of the lower epidermis. Characteristics of root and aerial part powders, such as fragments of epidermal and parenchymatous cells, fragments of spiral xylem vessels, and fragments of scalariform xylem vessels, were found in both of these powders. Moreover, the moisture content, total ash value, and acid-insoluble ash value of the powders are parameters that meet general standards according to regulations on raw material purity. Carotenoids, fatty acids, essential oils, flavonoids, tannins, coumarins, alkaloids, triterpenoids, amino acids, and carbohydrates were present in the *C. flavus* roots and aerial parts. The microscopic morphological characteristics, physicochemical parameters, and chemical composition are the highlights of this study. This specific information can be used to enrich new knowledge that was previously unknown, as well as a monograph to accurately identify this species, specifically *C. flavus*.

ACKNOWLEDGEMENTS

The authors wish to thank researchers supporting project number (187/2023/HĐ-ĐHYD) at University of Medicine and Pharmacy at Ho Chi Minh City, Vietnam. Funding information: This research was funded by University of Medicine and Pharmacy at Ho Chi Minh City under grant number 187/2023/HĐ-ĐHYD.

REFERENCES

Alamgir ANM. 2017. Pharmacognostical Botany: Classification of Medicinal and Aromatic Plants (MAPs), Botanical Taxonomy,

Morphology, and Anatomy of Drug Plants. In: Therapeutic Use of Medicinal Plants and Their Extracts. Prog Drug Res. Springer, Cham 1 (73): 177-293. DOI: 10.100-7/978-3-319-63862-1_6.

Anu S, Navas M, Dan M. 2020. Morpho-anatomical characterisation of the rhizomes of ten species of *Curcuma* L. (Zingiberaceae) from South India. J Spices Aromat Crops 29 (1): 38-47. DOI: 10.25081/josac.2020.v29.i1.6243.

Ariffin S, Azzeme AM, Hasbullah NI, Nawahwi MZ, Zemry IHB. 2023. Preliminary phytochemical screening of medicinal herb, SAMBAU PAYA (*Chloranthus erectus*). Mater Today: Proc 88 (2): 6-9. DOI: 10.1016/j.matpr.2023.01.365.

Carlquist S. 1992. Wood anatomy and stem of *Chloranthus*; summary of wood anatomy of Chloranthaceae, with comments on relationships, vessellessness, and the origin of monocotyledons. IAWA J 13 (1): 3-16. DOI: 10.1163/22941932-90000556.

Carpenter KJ. 2005. Stomatal architecture and evolution in basal angiosperms. Am J Bot 92 (10): 1595-1615. DOI: 10.3732/ajb.92.10.1595.

Chang-heng Z, Yong-xiang W, Zhi-bing W, Meng-xue W, Ya-li W, Tian-zhong C, Xing S. 2020. Effect of different drying methods on composition and biological activities of essential oils from *Chloranthus spicatus* flowers. Nat Prod Res Dev 32 (6): 1030-1037. DOI: 10.16333/j.1001-6880.2020.6.017.

Eklund H, Doyle JA, Herendeen PS. 2004. Morphological phylogenetic analysis of living and fossil Chloranthaceae. Intl J Plant Sci 165 (1): 107-151. DOI: 10.1086/380987.

FOC. 2024. *Chloranthus* Swartz. Flora of China. http://www.efloras.org/florataxon.aspx?flora_id=2&taxon_id=106776

Guo YQ, Zhao JJ, Li ZZ, Tang GH, Zhao ZM, Yin S. 2016. Natural nitric oxide (NO) inhibitors from *Chloranthus japonicus*. Bioorg Med Chem Lett 26 (13): 3163-3166. DOI: 10.1016/j.bmcl.2016.04.081.

Iqbal E, Salim KA, Lim LB. 2015. Phytochemical screening, total phenolics and antioxidant activities of bark and leaf extracts of *Goniothalamus velutinus* (airy shaw) from Brunei Darussalam. J King Saud Univ Sci 27 (3): 224-232. DOI: 10.1016/j.jksus.2015.02.003.

Kang J, Li N, Yuan Q, Wang Z. 2010. Morphological structure of vegetative organs and histochemical localization in *Chloranthus japonicus* Sieb. Acta Bot Boreal-Occid Sin 30 (12): 2412-2416.

Kaskoos RA, Ahamad J. 2014. Evaluation of pharmacognostic features of aerial parts of *Andrographis paniculata* Wall. J Pharmacogn Phytochem 3 (1): 1-5.

Kong HZ. 2001. Comparative morphology of leaf epidermis in the Chloranthaceae. Bot J Linn Soc 136 (3): 279-294. DOI: 10.100EVbojl.2001.0442.

Li N, Kang J, Yuan Q, Wang Z. 2011. Morphological structure of vegetative organs and histochemical localization in *Chloranthus multistachys* Pei. Plant Sci J 29 (4): 507-511.

Liu DT, Cai L, Chen G. 2019. *Chloranthus flavus* (Chloranthaceae), a new species from Guangxi, China. Phytotaxa 391 (4): 273-276. DOI: 10.11646/phytotaxa.391.4.6.

Liu YY, Li YZ, Huang SQ, Zhang HW, Deng C, Song XM, Wang W. 2022. Genus *Chloranthus*: A comprehensive review of its phytochemistry, pharmacology, and uses. Arab J Chem 2022: 104260. DOI: 10.1016/j.arabjc.2022.104260.

Lu YB, Huang ZP, Qin XM, Zhang Q. 2022. Combination of *Chloranthus flavus* into *C. nervosus* based on morphological and molecular evidence. Phytotaxa 564 (2): 230-238. DOI: 10.11646/phytotaxa.564.2.6.

Luan DT, Van Chen T, Nguyen DD, Truong QC, Thang KH, Nhi NTT, Triet NT. 2022. Morphological, physicochemical, and phytochemical characterization of *Camellia dormoyana* (Pierre) Sealy from Vietnam. Biodiversitas 23 (11): 5869-5883. DOI: 10.13057/biodiv/d231141.

Ministry of Health. 2017. Vietnamese Pharmacopoeia V. Medical Publishing House. Ha Noi, Vietnam.

Mrozek-Szetela A, Rejda P, Wińska K. 2020. A review of hygienization methods of herbal raw materials. Appl Sci 10 (22): 8268. DOI: 10.3390/app10228268.

Muyumba NW, Mutombo SC, Sheridan H, Nachtergael A, Duez P. 2021. Quality control of herbal drugs and preparations: The methods of analysis, their relevance and applications. Talanta Open 4: 100070. DOI: 10.1016/j.talo.2021.100070.

Nhi NTT, Chen TV, Lam DNX, Nguyen DD, Dinh QD, Linh NHK. 2023. Morphological and anatomical studies of *Conamomum vietnamense* NS. Lý & T.S. Hoang: An endemic plant from Vietnam. Biodiversitas 24 (9): 5022-5034. DOI: 10.13057/biodiv/d240946.

Nunes TD, Zhang D, Raissig MT. 2020. Form, development and function of grass stomata. Plant J 101 (4): 780-799. DOI: 10.1111/tpj.14552.

Osman AG, Raman V, Haider S, Ali Z, Chittiboyina AG, Khan IA. 2019. Overview of analytical tools for the identification of 3 adulterants in commonly traded herbs and spices. J AOAC Intl 102 (2): 376-385. DOI: 10.5740/jaoacint.18-0389.

POWO. 2024a. Chloranthaceae R.Br. ex Sims. Plants of the World Online. Kew Science. https://powo.science.kew.org/taxon/urn:lsid:ipni.org:names:77126698-1.

POWO. 2024b. *Chloranthus* Sw. Plants of the World Online. Kew Science. https://powo.science.kew.org/taxon/urn:lsid:ipni.org:names:7052-1

Segev R, Nannapaneni R, Sindurakar P, Kim H, Read H, Lijek S. 2015. The effect of the stomatal index on the net rate of photosynthesis in the leaves of *Spinacia oleracea*, *Vinca minor*, *Rhododendron* spp., *Epipremnum aureum*, and *Hedera* spp. J Emerg Investig 20: 1-5. DOI: 10.59720/15-005.

Srivastava S, Misra A. 2018. Quality Control of Herbal Drugs: Advancements and Challenges. In: Singh B, Peter K (eds). New Age Herbals: Resource, Quality and Pharmacognosy. Springer, Singapore 2018: 189-290. DOI: 10.1007/978-981-10-8291-7_10.

Thang TD, Dai DN, Ogunwande IA. 2016. Composition of essential oils from *Chloranthus elatior* and *Ch. spicatus* from Vietnam. Chem Nat Compd 52: 149-151. DOI: 10.1007/s10600-016-1575-x.

Tran CV, Vo TM, Bui PT, Duong DNP, Duong LXN, Dinh DQ, Hien NTT. 2023. Phytochemical screening, antioxidant activity and α-glucosidase inhibitability of *Bauhinia x blakeana* Dunn. leaf and flower extracts from Vietnam. Trop J Nat Prod Res 7 (4): 2737-2743. DOI: 10.26538/tjnpr/v7i4.11.

Van Chen T, Lam DNX, Thong CLT, Nguyen DD, Nhi NTT, Triet NT. 2022. Morphological characters, pharmacognostical parameters, and preliminary phytochemical screening of *Curcuma sahuynhensis* Škorničk. & NS. Lý in Quang Ngai Province, Vietnam. Biodiversitas 23 (8): 3907-3920. DOI: 10.13057/biodiv/d230807.

Wang AR, Song HC, An HM, Huang Q, Luo X, Dong JY. 2015. Secondary metabolites of plants from the genus *Chloranthus*: chemistry and biological activities. Chem Biodivers 12 (4): 451-473. DOI: 10.1002/cbdv.201300376.

Wang XJ, Yu SZ, Xin JL, Pan LL, Xiong J, Hu JF. 2022. Further terpenoids from the Chloranthaceae plant *Chloranthus multistachys* and their anti-neuroinflammatory activities. Fitoterapia 156: 105068. DOI: 10.1016/j.fitote.2021.105068.

WHO [World Health Organization]. 2011. Quality Control Methods for Medicinal Plant Materials. Geneva: WHO Press.

WHO [World Health Organization]. 2018. Fifty-second report of the WHO Expert Committee on Specifications for Pharmaceutical Preparations. WHO Technical Report Series, No. 1010.

Zhang M, Liu D, Fan G, Wang R, Lu X, Gu Y, Shi QW. 2016. Constituents from Chloranthaceae plants and their biological activities. Heterocyclic Commun 22 (4): 175-220. DOI: 10.1515/hc-2016-0084.

Zhuo ZG, Wu GZ, Fang X, Tian XH, Dong HY, Xu XK, Shen YH. 2017. Chlorajaponols A-F, sesquiterpenoids from *Chloranthus japonicus* and their in vitro anti-inflammatory and anti-tumor activities. Fitoterapia 119: 90-99. DOI: 10.1016/j.fitote.2017.04.009.